1.D.1 Nuclear Physics 73 (1965) 1—24; © North-Holland Publishing Co., Amsterdam

EFFECTIVE INTERACTIONS FOR THE 1p SHELL

S. COHEN and D. KURATH
Argonne National Laboratory, Argonne, Illinois †

Received 9 March 1965

Abstract: Effective interactions for the 1p shell are obtained by fitting energy data about nuclear levels. Magnetic dipole moments and probabilities for M1 gamma transitions and beta decay are calculated with the resultant wave functions. Comparison of such quantities with experiment provides an important check on the validity of the picture. The properties of the interaction are compared with those found in an earlier calculation and are also compared with the interaction deduced from nucleon-nucleon scattering. For consistency with the scattering potential, one must include a term proportional to $(\boldsymbol{\sigma}_1 \cdot \boldsymbol{l})(\boldsymbol{\sigma}_2 \cdot \boldsymbol{l})$ as was introduced by Hamada and Johnston.

1. Introduction

The 1p shell has been a testing ground for nuclear models since the beginning of studies in nuclear structure. This is due to the simplicity of the configuration and to the accumulated wealth of experimental evidence. Early efforts consisted in choosing particular forms of two-body interaction and varying the difference between the $1p_{\frac{3}{2}}$ and $1p_{\frac{1}{2}}$ single-particle energies [1]). Another procedure [2]), adopted from atomic spectroscopy, is to consider the matrix elements of the two-body interaction as parameters. If there is a sufficient amount of experimental information, one can test the validity of the assumption that the states considered all arise from 1p configurations and can obtain numerical values for the integrals of the two-body interaction in the process of fitting the energies.

For the 1p shell there are fifteen matrix elements for the two-body interaction and two single-particle energies. Experiments provide something like fifty energy determinations of states with reasonably certain assignment of angular momentum and parity. However, these are not necessarily independent pieces of information so the problem of fitting parameters to the data is not greatly overdetermined. Furthermore, one must choose carefully to be reasonably certain that the states selected are well described by the 1p-shell configuration. As a test for the consistency of the picture, one should check whether the wave functions that result from such an energy fit lead to values in agreement with experiment for other observables which depend primarily on the 1p-shell nature of the states. Magnetic dipole moments, M1 transitions and Gamow-Teller beta decays are pertinent to this question.

† Work performed under the auspices of the U.S. Atomic Energy Commission.

The number of independent two-body matrix elements is reduced to eleven if the radial wave functions for $1p_{\frac{1}{2}}$ and $1p_{\frac{3}{2}}$ are the same and if one requires the interaction to be of the charge-independent non-relativistic form such as is used to analyse nucleon-nucleon scattering below 300 MeV. Since it will be shown that such a restricted form of interaction fits many of the data quite well, it is of interest to compare the resulting integrals of the interaction with what one would expect from the free-nucleon interaction.

The first part of the paper discusses the method of calculation and selection of data. Then the results are presented and compared both with experiment and with a similar calculation by Amit and Katz [3]). Our results differ markedly from those of Amit and Katz. Finally, the numerical results are interpreted in terms of the phenomenological potential obtained from nucleon-nucleon scattering.

2. Computational Procedure and Data Selection

The calculation was carried out on the CDC-3600 computer by use of the Argonne system of shell-model programs [4]). The parameters were determined by making a least-squares fit to the selected experimental energies, the method being an adaptation of a variable-metric method for minimization in a multidimensional space [5]).

The experimental quantities selected were the energy differences between the excited states and the ground state for each nucleus, as well as the binding energy of each ground state with respect to the $(1s)^4$ core. This procedure has been followed in an attempt to minimize the effect of ignoring configuration admixtures from outside the 1p shell. It is hoped that the admixture effects tend to cancel in the energy differences. Since the number of differences outweighs the number of ground states by a factor of about three in the fitting procedure, the resultant interaction may be more nearly appropriate for the 1p shell.

The Coulomb contribution to the binding energy was not calculated for each state since it will not have any appreciable effect on the energy differences. For the binding energies of the ground states, the Coulomb contributions Δ_z were estimated from observed energy differences between mirror nuclei. The numerical values of Δ_z are given in column 2 of table 1, where they are subtracted from the experimental differences of binding energy to obtain quantities for comparison with the calculated nuclear binding energies with respect to the $(1s)^4$ core.

The low-lying excited states for which there is a reasonably certain experimental identification were naturally selected as those most likely to be represented well by 1p-shell configurations. The lowest states having $T = T_z + 1$ were also included for even-mass nuclei since these isobaric-spin analogue states should also arise chiefly from the 1p shell. Only two well-known states were omitted. One is the 4^+ level of Be^8 which is so broad that almost any interaction will predict a level in this general vicinity. The other is the 0^+ excited state of C^{12} at 7.65 MeV; including it produces a large increase in the χ^2 of the over-all fit. An argument for believing that this state

contains a large component from outside the 1p shell will be presented later. The states contained in the energy fit are indicated by heavy lines in the experimental spectra on the left in figs. 1–9.

The matrix elements of the two-body interaction can be written in the *j-j* representation form $\langle j_1 j_2 JT|V|j_3 j_4 JT\rangle$, where the single-particle functions j_i are either $1p_{\frac{3}{2}}$ or $1p_{\frac{1}{2}}$. There are ten diagonal matrix elements [wherein $(j_1 j_2)$ equals $(j_3 j_4)$] and five non-diagonal elements for the 1p shell. The process of determining numerical values for these matrix elements by fitting a set of energy levels involves no assumptions about the single-particle functions except that they are constant over the range of nuclear levels in the fit. The radial wave functions for $1p_{\frac{3}{2}}$ and $1p_{\frac{1}{2}}$ need not be the same and this may be an important freedom for the lighter nuclei in the shell.

However, for a large fraction of the shell it will prove to be a reasonable approximation to assume that the radial wave functions are the same. It is then convenient to consider the interaction matrix elements in the *LS*-representation form $\langle LSJT|V|\bar{L}\bar{S}JT\rangle$. Here L represents the resultant orbital angular momentum of two 1p nucleons, and the orbital wave function has the symmetry $(-1)^L$ under permutation of the nucleons. Again there are ten diagonal matrix elements (wherein LS equals $\bar{L}\bar{S}$) and five non-diagonal ones. However, four of the five non-diagonal elements connect an orbital wave function with $L = 1$ to a wave function of even L. Phenomenological potentials derived from nucleon-nucleon scattering are symmetric under permutation of the spatial coordinates and lead to vanishing of the non-diagonal matrix elements between states of opposite spatial symmetry. Thus for making an energy fit under these conditions there are only eleven parameters from the interaction.

The two approximations are therefore the 17-parameter case with general two-body matrix elements (hereafter denoted as 2BME) and the 13-parameter case with a potential in the *LS* representation (hereafter denoted as POT).

3. Results and Comparison of Energy Fits

In order to minimize the effects of size variation near the beginning of the shell and configuration mixing at the upper end of the shell, a first attempt was made by fitting only the data from $A = 8$ through $A = 12$ as well as the splitting of the single-hole levels found in $A = 15$. While the 2BME fit was naturally better than the POT fit, this improvement depended on rather unlikely values for the matrix elements involving only $1p_{\frac{1}{2}}$ nucleons. Furthermore, the spectra predicted for the $A = 13$ and $A = 14$ nuclei were quite similar to the experimental ones for the POT case but were very different in the 2BME case.

Therefore, 35 data from $A = 8$ through $A = 16$ were fitted for both the POT and the 2BME parameterizations. The fits from these two cases are very similar, as one can see from table 2 where the squares of the energy deviation from experiment are listed in columns 3 and 4. The root-mean-square energy deviations are 430 keV for the POT and 400 keV for the 2BME case. Similar fits were tried for the 44 data from

$A = 6$ through $A = 16$. These lead to much poorer over-all fits, giving root-mean-square deviations of 650 keV for POT and 570 keV for 2BME with the major part of the deviation coming from $A = 6$–8. The 2BME case is listed on the right in table 2.

TABLE 1

Nuclear binding energies for the ground states with respect to the ground state of He^4

Nucleus	$\Delta_{exp} - \Delta_z = \Delta_{nucl}$ (MeV)	Δ_{8-16}(POT) (MeV)	Δ_{8-16}(2BME) (MeV)	Δ_{6-16}(2BME) (MeV)
Li^6	3.69 + 1.00 = 4.69	(5.43)	(5.79)	5.55
Li^7	10.95 + 1.00 = 11.95	(14.61)	(14.38)	13.67
Be^8	28.20 + 2.64 = 30.84	31.13	30.95	30.28
Be^9	29.86 + 2.64 = 32.50	32.54	32.37	31.98
B^{10}	36.45 + 4.61 = 41.06	41.50	41.44	41.03
B^{11}	47.91 + 4.61 = 52.52	52.82	52.94	52.42
C^{12}	63.87 + 7.23 = 71.10	71.05	71.18	71.07
C^{13}	68.82 + 7.23 = 76.05	75.23	75.39	75.24
N^{14}	76.36 + 10.24 = 86.60	85.93	86.00	86.16
O^{15}	83.66 + 13.83 = 97.49	97.53	97.47	97.66
$O^{15*} - O^{15}$	6.25	6.36	6.30	7.02
O^{16}	99.32 + 13.83 = 113.15	113.82	113.69	113.78

In column 2, Δ_{exp} is the experimental difference between the total binding energies and Δ_z is the Coulomb contribution. The three columns on the right contain calculated values, fitted over the indicated mass range with either the potential form or with two-body matrix elements as parameters.

TABLE 2

Contribution to χ^2 from each mass number A in the energy fits

A	N	$\Sigma[E - E_{exp}]^2$ (8–16)POT	(8–16)2BME	(6–16)2BME
6	6			3.02
7	3			3.32
8	4	1.39	1.13	1.82
9	2	0.22	0.10	0.29
10	9	0.80	0.82	0.71
11	6	1.91	1.85	2.33
12	5	0.46	0.45	0.60
13	3	0.69	0.44	0.74
14	3	0.70	0.39	0.45
15	2	0.02	0.00	0.63
16	1	0.44	0.30	0.40
total		6.63	5.48	14.32
$(E - E_{exp})_{rms}$(MeV)		0.43	0.40	0.57

Column 2 lists the number N of pieces of data. The sum of the squared energy deviations is given at the bottom, together with the root-mean-square energy deviations in the fits.

Figs. 1–9 show the energy differences for the three cases of table 2, together with the experimental energy data. The levels included in the fit are indicated by heavy lines in these figures. Since only excitation energies were calculated for excited states, the

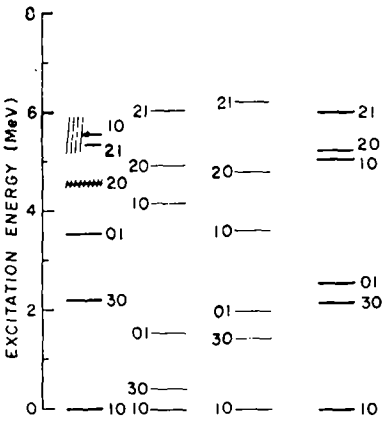

Fig. 1. The level scheme of Li^6 with levels identified by (JT). Column 1 is experimental, column 2 results from the (8–16)POT case, column 3 results from the (8–16)2BME case, and column 4 results from the (6–16)2BME case. Heavy lines with identification on the right were included in the energy fits. Light lines in the calculations with identification on the left arise from the parameters determined by the energy fits.

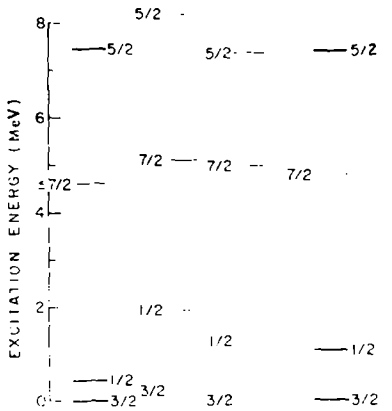

Fig. 2. The level scheme of Li^7. All levels are identified by J and have $T = \frac{1}{2}$ unless otherwise noted. Column 1 is experimental, column 2 results from the (8–16)POT case, column 3 results from the (8–16)2BME case, and column 4 results from the (6–16)2BME case. Heavy lines with identification on the right were included in the energy fits. Light times in the calculations with identification on the left arise from the parameters determined by the energy fits.

figures are drawn with the same ground-state energies. The calculated ground-state binding energies are listed in table 1, which also contains the excitation energy of the single excited state which is considered for $A = 15$.

The squares of the energy deviations have an exponential distribution. The average contribution from the ground state binding energies is not appreciably different from the general average. However, there are a few large contributions such as those from the ground states of C^{13}, N^{14} and particularly Li^7. In fact, as is clear from table 2,

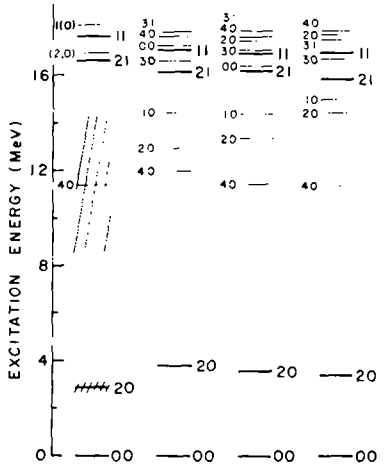

Fig. 3. The level scheme of Be^8. See caption of fig. 1 for details.

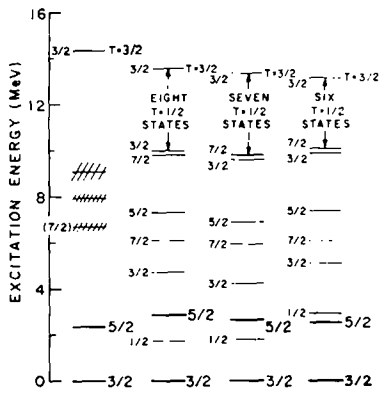

Fig. 4. The level scheme of Be^9. See caption of fig. 2 for details.

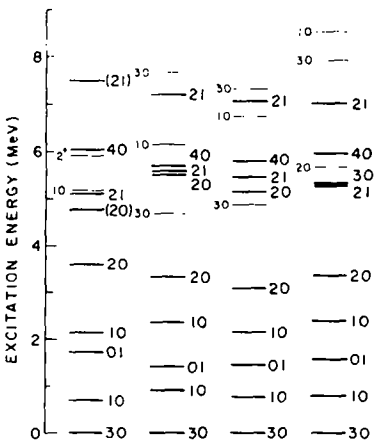

Fig. 5. The level scheme of B^{10}. See caption of fig. 1 for details.

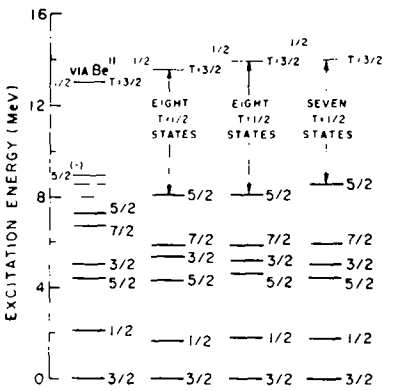

Fig. 6. The level scheme of B^{11}. See caption of fig. 2 for details.

the A = 6–16 case has abnormally large contributions from the low end of the shell. This feature is even stronger in the POT treatment of A = 6–16. The reason for this behaviour may well be that the assumption of constant matrix elements is too severe a restriction to allow a fit to the entire shell, particularly to the lower end of the shell where the nucleon orbits may be changing size appreciably as more 1p nucleons are

added. The effective interaction for the Li isotopes may have considerably different features. However, the change is probably not drastic, since, as is seen in figs. 1 and 2, the spectra of Li^6 and Li^7 are crudely similar to observation even with the interactions determined in the $A = 8$–16 fits.

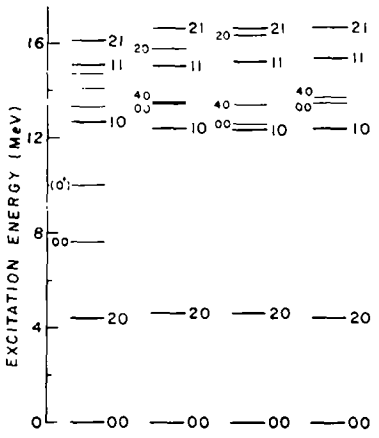

Fig. 7. The level scheme of C^{12}. See caption of fig. 1 for details.

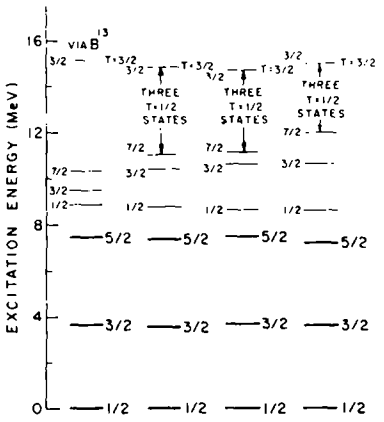

Fig. 8. The level scheme of N^{13}. See caption of fig. 2 for details.

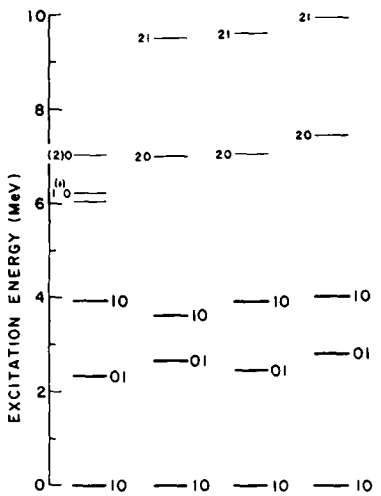

Fig. 9. The level scheme of N^{14}. See caption of fig. 1 for details.

4. Tests of the Resultant Wave Functions

4.1. GENERAL MOTIVATION

Once an energy fit has been made, one has an effective interaction which can then be used to calculate the complete spectra for the 1p configurations. This gives levels

which were not used in the energy fit, and these are indicated by the light lines in the theoretical spectra of figs. 1–9. The wave functions extracted are appropriate for calculating other quantities that depend on the 1p-shell nature of these states. The observable quantities best suited for testing these wave functions are the magnetic dipole moments, Gamow-Teller beta decays and M1 gamma transitions. This is because the operators for these quantities connect single-particle 1p functions only to themselves † and hence are less sensitive to admixtures of other configurations.

TABLE 3

Magnetic dipole moments (nuclear magnetons) for the ground states that are identified in column 1

Nucleus	I	Inglis (a/K)	(8–16)POT	(8–16)2BME	(6–16)2BME	Exp
Li^6	1	0.875(1.5)			0.833	0.822
Li^7	$\frac{3}{2}$	3.134(1.5)			3.170	3.256
Li^8	2	1.326(1.5)	1.367	1.377	1.556	1.653
Be^9	$\frac{3}{2}$	−0.975(3.0)	−1.270	1.324	−1.297	−1.177
B^{10}	3	1.768(4.5)	1.812	1.812	1.816	1.801
B^{11}	$\frac{3}{2}$	1.910(4.5)	2.631	2.488	2.505	2.688
B^{12}	1	0.429(4.5)	0.761	0.599	0.437	
C^{13}	$\frac{1}{2}$	0.670(6.0)	0.757	0.700	0.701	0.702
N^{14}	1	0.347(6.0)	0.331	0.326	0.331	0.404

Column 2 lists the results of the calculation with the Inglis mixture and values of (a/K) as indicated in parentheses. The other columns are calculated with wave functions resulting from the indicated energy fits. The experimental value is on the right.

Therefore such quantities provide good tests for the 1p structure of the wave functions. The calculated quantities are also useful as indications of changes in the wave functions. This feature is employed in tables 3–5 which list the results for the three energy fits as well as for an earlier calculation [9]). The old calculation used a purely central-force interaction, suggested by Inglis [10]), and varied the single-particle level splitting as a function of mass number. The magnetic dipole moments are listed in table 3, the values of log ft are listed in table 4, and the M1 transition strengths are given in table 5.

The over-all comparison indicates that the wave functions of the low-lying states are not appreciably different from those which resulted from the old calculation [9]) despite the fact that the interaction is considerably different. This has also been confirmed in a number of cases by comparing the wave functions directly.

Furthermore it is encouraging to note that where there are changes, the present calculations usually are closer to experimental observation than the old one. The evidence supports the effective 1p-shell interactions as being reasonable. Particular points of interest are discussed in the following comments arranged according to mass number.

† This is not true for transitions induced by inelastic scattering of electrons with high momentum transfer.

4.2. THE SPECTRA OF $A = 6, 7$

The spectra resulting from the (6–16) 2BME calculation, shown on the right of figs. 1 and 2, are not very close to experiment. In particular, the binding energy of Li^7 is difficult to fit, differing by 1.7 MeV from the experimental value. The resulting wave functions are all very close to those of LS coupling, so that the magnetic moments, the beta transition and the M1 transitions agree well with experiment and with older calculations.

TABLE 4

Values of log ft for allowed Gamow-Teller beta decays

$A(I_0T_0) \to I$	Inglis(a/K)	(8–16)POT	(8–16)2BME	(6–16)2BME	Exp.	Ref.
6(0 1) → 1	2.87 (1.5)			2.89	2.91	[6]
8(2 1) → 2	5.67 (1.5)	4.77	5.04	5.26	5.7	[6]
9($\frac{3}{2}$ $\frac{3}{2}$) → $\frac{3}{2}$	5.06	4.68	4.75	5.12	5.5	[7]
→ $\frac{5}{2}$	5.05	4.99	4.95	5.10	4.7	
→ $\frac{1}{2}$	5.14 (3.0)	4.67	4.92	5.38		
→ $\frac{3}{2}$*	4.89	4.73	5.33	6.65		
→ $\frac{5}{2}$*	5.86	5.06	4.71	4.42		
10(0 1) → 1	3.79 (4.5)	2.91	2.94	2.91	3.03	[6]
→ 1*	3.01	3.83	3.72	4.10		
11($\frac{1}{2}$ $\frac{3}{2}$) → $\frac{3}{2}$	3.89	3.98	3.93	3.89	6.77	[6]
→ $\frac{1}{2}$	6.49 (4.5)	7.30	6.49	6.03	6.63	
→ $\frac{3}{2}$*	6.42	>7.60	7.30	6.58	≧8.2	
12(1 1) → 0	4.13	4.11	4.08	4.11	4.1	[6]
→ 2	4.80	4.80	4.98	5.06	5.1	
→ 0*	3.60	3 52	3 54	3.51		
→ 1	3.66	3.61	3.63	3.64		
13($\frac{3}{2}$ $\frac{3}{2}$) → $\frac{1}{2}$	3.79	3.93	3.89	3.88	4.01	[8]
→ $\frac{3}{2}$	4.38 (6.0)	4.68	4.59	4.78	4.53	
→ $\frac{5}{2}$	4.60	5.18	5.98	5.23	≧4.7	
14(0 1) → 1	4.01 (6.0)	4.45	5.42	4.92	9.03	[6]

Transitions are identified in column 1; the final isobaric spin is always $T_0 - 1$. Values for various calculations are given in columns 2–5, and experimental values are listed on the right.

4.3. THE SPECTRUM OF $A = 8$

The energy fit to four levels in Be^8 is only moderately good. Also, fig. 3 exhibits the calculated second (20) and first(10) levels as lying in a region in which no levels are known experimentally. However, in going from the (8–16) fits to the (6–16)2BME case, these levels rise nearer to the region where they would be expected from experiment. This indicates that parameters more appropriate to $A = 6$ and 7 may be needed for $A = 8$. The magnetic moments of Li^8 and the beta-decay probabilities are also nearer to experiment for the (6–16)2BME case.

The M1 transition strengths are similar to those of the old calculation with a spin-orbit coupling parameter value of $(a/K) \approx 1.5$. A value nearer $(a/K) = 3$ has been shown to be preferable for the (11) → (00) transition [11], for which the experimental

TABLE 5

Values of M1 transitions strengths calculated for various cases

I_1T_1	I_2T_2	Inglis(a/K)	(8–16)POT	(8–16)2BME	(6–16)2BME
		(1.5)	$A = 6$		
1 0	0 1	69.4			62.9
	1 0*	0.003			0.14
	2 0	0.001			0.05
	2 1	0.85			2.71
		(1.5)	$A = 7$		
$\frac{3}{2}\ \frac{1}{2}$	$\frac{1}{2}\ \frac{1}{2}$	37.7			37.2
	$\frac{1}{2}\ \frac{1}{2}$*	0.34			0.04
	$\frac{3}{2}\ \frac{1}{2}$*	0.36			1.12
	$\frac{5}{2}\ \frac{1}{2}$	0.07			0.02
	$\frac{5}{2}\ \frac{1}{2}$*	0.42			0.98
	$\frac{1}{2}\ \frac{3}{2}$	0.004			0.12
	$\frac{3}{2}\ \frac{3}{2}$	1.45			2.15
	$\frac{5}{2}\ \frac{3}{2}$	3.27			3.38
		(1.5)	$A = 8$		
1 1	0 0	1.90	2.44	1.42	2.44
	1 0	19.8	34.6	35.0	22.3
	2 0	0.48	0.94	0.32	0.42
	2 0*	48.1	48.6	50.7	34.0
2 1	1 0	52.7	43.9	43.4	38.5
	2 0	1.36	7.65	4.81	3.82
	2 0*	156.4	162.7	162.3	147.1
		(3.0)	$A = 9$		
$\frac{3}{2}\ \frac{1}{2}$	$\frac{1}{2}\ \frac{1}{2}$	18.7	18.6	19.4	19.6
	$\frac{1}{2}\ \frac{1}{2}$*	1.70	1.36	0.93	1.60
	$\frac{3}{2}\ \frac{1}{2}$*	9.91	6.43	4.91	4.69
	$\frac{5}{2}\ \frac{1}{2}$	13.1	9.93	8.62	9.13
	$\frac{5}{2}\ \frac{1}{2}$*	1.51	0.03	0.01	0.02
	$\frac{1}{2}\ \frac{3}{2}$	4.87	0.60	0.60	1.75
	$\frac{3}{2}\ \frac{3}{2}$	4.75	7.87	7.30	4.65
	$\frac{5}{2}\ \frac{3}{2}$	0.21	0.33	0.19	0.07
		(4.5)	$A = 10$		
3 0	2 0	0.31	0.13	0.04	0.000
	2 0*	0.37	0.51	0.60	0.66
	3 0*	0.12	0.000	0.000	0.000
	4 0	0.33	0.20	0.20	0.17
	2 1	0.46	8.32	5.93	1.09
	2 1*	81.7	103.5	103.3	103.2
	2 1**	19.5	6.46	10.6	16.3
	3 1	44.6	33.9	33.6	29.6
	4 1	7.15	2.93	2.82	1.98
0 1	1 0	14.1	51.7	47.8	52.8
1 0*	1 0	0.14	0.15	0.18	0.06
	0 1	39.8	11.5	14.5	8.80

TABLE 5 (continued)

I_1T_1	I_2T_2	Inglis(a/K)	(8–16)POT	(8–16)2BME	(6–16)2BME
2 0	3 0	0.31	0.13	0.04	0.000
	1 0	0.30	0.05	0.06	0.015
	1 0*	0.04	0.45	0.41	0.41
3 0*	3 0	1.12	0.000	0.000	0.000
	2 0	0.20	0.47	0.52	0.59
2 1	3 0	0.46	8.32	5.93	1.09
	1 0	67.9	0.08	0.27	0.001
	1 0*	1.34	45.9	49.5	70.5
	2 0	23.2	36.6	56.5	76.9
	3 0*	92.4	109.5	111.3	129.8
2 0*	3 0	0.37	0.51	0.60	0.66
	1 0	0.20	0.002	0.01	0.03
	1 0*	0.02	0.42	0.50	0.03
	2 0	0.03	0.003	0.01	0.01
	3 0*	0.21	0.09	0.02	0.000
	2 1	49.0	44.7	25.2	3.02
4 0	3 0	0.33	0.20	0.20	0.17
	3 0*	0.26	0.003	0.000	0.001
			(4.5) $A = 11$		
$\frac{3}{2}\ \frac{1}{2}$	$\frac{1}{2}\ \frac{1}{2}$	9.28	16.8	15.7	15.1
	$\frac{1}{2}\ \frac{1}{2}$*	1.29	0.50	0.38	0.23
	$\frac{3}{2}\ \frac{1}{2}$*	28.5	22.1	23.1	22.7
	$\frac{3}{2}\ \frac{1}{2}$**	0.59	0.14	0.34	0.06
	$\frac{5}{2}\ \frac{1}{2}$	20.1	13.3	13.4	13.1
	$\frac{5}{2}\ \frac{1}{2}$*	6.05	6.52	7.77	9.35
	$\frac{5}{2}\ \frac{1}{2}$**	4.98	0.10	0.56	0.68
	$\frac{1}{2}\ \frac{3}{2}$	13.5	10.0	11.5	12.5
	$\frac{3}{2}\ \frac{3}{2}$	10.8	11.3	11.4	12.7
	$\frac{5}{2}\ \frac{3}{2}$	1.00	2.50	1.95	1.57
$\frac{3}{2}\ \frac{1}{2}$*	$\frac{3}{2}\ \frac{1}{2}$	28.5	22.1	23.1	22.7
	$\frac{1}{2}\ \frac{1}{2}$	21.2	13.9	15.6	16.6
	$\frac{5}{2}\ \frac{1}{2}$	38.0	48.0	47.7	46.7
$\frac{5}{2}\ \frac{1}{2}$*	$\frac{3}{2}\ \frac{1}{2}$	6.05	6.52	7.77	9.35
	$\frac{5}{2}\ \frac{1}{2}$	5.22	2.38	0.18	0.20
	$\frac{3}{2}\ \frac{1}{2}$*	0.59	0.21	0.14	0.50
	$\frac{7}{2}\ \frac{1}{2}$	53.0	11.2	16.8	14.2
$\frac{7}{2}\ \frac{1}{2}$	$\frac{5}{2}\ \frac{1}{2}$	0.002	0.35	0.23	0.39
			(4.5) $A = 12$		
1 1	0 0	9.89	9.69	10.6	10.2
	0 0*	25.8	31.4	30.1	30.9
	1 0	32.7	37.1	35.9	35.1
	2 0	0.90	1.18	0.60	0.37
2 1	1 0	1.89	9.91	7.57	5.57
	1 1	1.79	3.59	4.86	5.65
	2 0	8.46	13.4	12.2	11.4

TABLE 5 (continued)

I_1T_1	I_2T_2	Inglis(a/K)	(8-16)POT	(8-16)2BME	(6-16)2BME
		(6.0)	$A = 13$		
$\frac{1}{2}\,\frac{1}{2}$	$\frac{1}{2}\,\frac{1}{2}$*	8.95	7.15	7.28	7.62
	$\frac{3}{2}\,\frac{1}{2}$	15.8	20.3	19.0	19.9
	$\frac{3}{2}\,\frac{1}{2}$*	9.09	3.52	5.21	4.54
	$\frac{3}{2}\,\frac{3}{2}$	23.4	16.7	18.0	18.4
		(6.0)	$A = 14$		
1 0	0 1	1.18	0.17	0.14	0.001
	1 0*	0.08	0.02	0.000	0.001
	2 1	57.9	60.9	62.4	62.0
1 0*	0 1	33.4	44.0	43.4	34.6

The quantity is $[2I_1+1]\Lambda_{M1}(I_1T_1 \to I_2T_2) = [2I_2+1]\Lambda_{M1}(I_2T_2 \to I_1T_1)$. The width in eV is given by $\Gamma_{M1}(I_1T_1 \to I_2T_2) = 2.76\times10^{-3}E^3\Lambda_{M1}(I_1T_1 \to I_2T_2)$, where E is the gamma energy in MeV. Odd-mass results refer to stable partner.

value is $3\Lambda_{M1}(11 \to 00) = 3.3$. The experimental strength for the branch to the lowest (20) state is $3\Lambda_{M1}(11 \to 20) = 2.8$. Comparing these values with the entries of table 5 shows the calculated values to be low. A point of interest is that table 5 shows the calculated transition strength to the next (20) state to be very large, so that interaction that mixes some of the (20)* with the (20) could remove the discrepancy.

4.4. THE SPECTRUM OF $A = 9$

The calculated spectra are quite similar to the old calculation, and questions raised in comparing with experiment are much the same as the ones given there. A new point concerns the $(\frac{3}{2}\,\frac{3}{2})$ state which, while not in the fit, is calculated to lie at about 13.4 MeV. Its observed position is 14.4 MeV. The M1 transition strength to this state, as measured by electron scattering [12]), is $4\Lambda_{M1}(\frac{3}{2}\,\frac{1}{2} \to \frac{3}{2}\,\frac{3}{2}) = 8\pm4$, which is in the range of values given for this transition in table 5.

A remaining unsolved question is the position of the lowest $(\frac{1}{2}\,\frac{1}{2})$ state, which has not been observed but which is seen from table 5 to have a large M1 transition strength and should be excited in electron-scattering experiments. It may be close to the $(\frac{5}{2}\,\frac{1}{2})$ state at 2.43 MeV and may thus account for the large transition strength found there in electron scattering [12]). The beta-decay values in table 4 indicate weak transitions as are observed: but the ratios do not agree with observation. However, weak transitions are very sensitive to the wave functions.

4.5. THE SPECTRUM OF $A = 10$

In this case the calculated spectrum fits the experiment quite well. A point of interest concerns the 4.77 MeV state which was at first given the probable assignment [6])

of (20) in the (8–16) calculations. However, the level was difficult to fit, and the spectra from the resultant interactions gave a (30) level in this region. Because of subsequent tentative information [13]) that the (30) assignment may be correct, the 4.77 MeV level was designated as (30) in the final calculations. The important change from the older calculation with the Inglis mixture concerns the nature of the two (10) states at 0.72 and 2.15 MeV. This is most striking in the beta decay of C^{10}, shown in table 4, where the two levels have in effect switched character and experiment supports the values of the present calculation. This change also affects the strong M1 transitions connecting these levels with the $T = 1$ levels at 1.74 and 5.16 MeV. Although the agreement between the predicted and observed branching ratios may be somewhat better than in the old calculations, these quantities are very sensitive to the wave functions and the restrictions imposed by the energy fit are not good enough to fix the branching ratios well.

4.6. THE SPECTRUM OF $A = 11$

The fit to the $A = 11$ spectrum is fair. The old difficulty of getting the lowest $\frac{7}{2}^-$ state as high as 6.76 MeV is still present. The lowest $T = \frac{3}{2}$ state, while not in the fit, lies in about the expected region of excitation. The magnetic moment is quite sensitive to the wave function and is near the experimental values. It should be pointed out that the old calculation [9]) was found to contain an error in the $(\frac{3}{2}\,\frac{1}{2})$ energy matrix, and the corrected value in table 3 is about 0.9 nuclear magnetons lower than the old result. The beta-decay results in table 4 show strong disagreement with the observed log ft for the transition to the ground state of B^{11}, and thus support the proposal [14, 15]) that the ground state of Be^{11} has positive parity. The general calculations of M1 transition strengths give results very similar to those of the old calculation.

4.7. THE SPECTRUM OF $A = 12$

The fit to the energy spectrum is reasonable. The values of log ft for the decay of B^{12} to the (00) and (20) states of C^{12} are close to the experimental observations. The calculated values of transition strength from the 15.1 MeV level (11) to the ground state are seen from table 5 to give $3A_{M1}(11 \rightarrow 00) \approx 10$, which is about 20 % below the latest [16]) experimental value.

4.8. THE SPECTRUM OF $A = 13$

The most interesting feature of the spectrum is the $\frac{5}{2}^-$ state at 7.4 MeV. In the early calculation with masses $A = 8$–12 only, the resultant POT interaction gave $\frac{5}{2}^-$ level at about 7 MeV. Since there is evidence [17]) that a $\frac{5}{2}^-$ level exists at 7.4 MeV in N^{13}, such a level was included in the fits. The $(\frac{3}{2}\,\frac{3}{2})$ level, the analogue to the B^{13} ground state, appears at about the right energy. Beta decays from this level agree well with observation.

A point of interest is that table 5 shows a large transition strength between the ground state of C^{13} and the $(\frac{3}{2}\ \frac{3}{2})$ state which should appear at about 15 MeV. This should show up strongly in inelastic electron scattering with a width of $\Gamma_{M1}(\frac{1}{2}\ \frac{1}{2} \rightarrow \frac{3}{2}\ \frac{3}{2}) \approx 80$ eV.

4.9. THE SPECTRUM OF $A = 14$

The major point of interest here concerns the beta decay of C^{14}, which has long been a difficulty for the shell model. From table 5 one sees that the logft for the (8–16) 2MBE case has increased by 1.4 over the old calculation with the Inglis mixture. Actually the use of logft values makes the disagreement with experiment look much worse than it is. A better criterion is to note that the square of the reduced matrix element for beta decay has dropped from 0.39 in the old calculation to 0.015 for the (8–16)2BME case. Actually changing the N^{14} ground state to one which has an overlap of 0.998 with the state from the latter case would produce the nearly exact cancellation indicated by experiment. Since small $(2s\ 1d)^2$ admixtures could also lead to the cancellation, the calculated value is really quite close to experiment.

4.10 USE OF TABLES 3–5

The numbers in tables 3–5 are exhibited in order to support the general validity of the model with the parameters resulting from the energy fit; they are not meant as a challenge to experimentalists to show what is wrong or which fit is better. Since it has been shown that the various calculated observables are often very sensitive to the wave functions, it would be better first to include the well-established data together with the energies in determining an interaction. It is likely that most of the beta-decay and M1 observables could be fitted without seriously altering the interaction.

5. Comparison with the Calculation of Amit and Katz

Amit and Katz [3]) have recently published a calculation which is in essence identical with the (8–16)2BME case. In order to compare the parameters of the two calculations, it is necessary to adjust for the fact that Amit and Katz calculated binding energies with respect to O^{16} rather than with respect to He^4 as in our cases. This is done by adding a constant amount (0.13 MeV) to all the diagonal matrix elements of their two-body interaction, and subtracting 1.06 MeV from both of their single-particle energies $\varepsilon_{\frac{1}{2}}$ and $\varepsilon_{\frac{3}{2}}$. This has no effect on their energy differences or their wave functions, and with these adjusted parameters we have reproduced all of the levels in figs. 1–4 of their paper. The numerical values of the parameters are listed in table 6 together with those resulting from the various cases in the present calculation. While these latter cases are fairly similar, they differ appreciably from the result of Amit and Katz, especially for the single-particle energies.

The difference in parameters results from the selection of data. Although the fit of Amit and Katz and the fit from the (8–16)2BME case both have root-mean-square

energy deviations of about 400 keV for about 35 pieces of information, only 25 are common to both fits. The remaining data contain four pieces of information that are fitted by Amit and Katz and are very poorly fitted in the (8–16)2BME case, and five pieces of information for which the reverse is true. These, which must contain the source of disagreement, will now be discussed.

TABLE 6

Parameters determined by the cases of the present calculation together with those from the (8-16)2BME calculation of Amit and Katz

$2(j_1+j_2)$	$2(j_3+j_4)$	J	T	(6–16)2BME	(8–16)POT	(8–16)2BME	Amit&Katz
6	6	0	1	−2.74	−3.33	−3.19	−4.12
6	6	2	1	−0.65	+0.09	−0.17	−1.28
6	6	1	0	−3.14	−3.44	−3.58	−5.50
6	6	3	0	−6.68	−7.27	−7.23	−5.64
6	4	2	1	−2.21	−1.74	−1.92	−1.71
6	4	1	0	+4.02	+3.21	+3.55	0
6	2	0	1	−5.32	−5.05	−4.86	+2.01
6	2	1	0	−1.09	+1.77	+1.56	0
4	4	1	1	+0.86	+0.73	+0.92	+2.68
4	4	2	1	−1.14	−1.14	−0.96	−0.38
4	4	1	0	−6.54	−6.56	−6.22	−8.82
4	4	2	0	−4.22	−4.06	−4.00	−3.67
4	2	1	0	+1.39	+1.20	+1.69	+1.89
2	2	0	1	+0.34	+0.24	−0.26	−2.27
2	2	1	0	−4.26	−4.29	−4.15	−3.79
$\varepsilon_{\frac{1}{2}}$				−2.27	+2.42	+1.57	−2.49
$\varepsilon_{\frac{3}{2}}$				+1.63	+1.13	+1.43	+2.25

The two-body matrix elements $\langle j_1 j_2 JT|V|j_3 j_4 JT\rangle$ are labelled by $(2j_1-2j_2)(2j_3+2j_4)JT$, and the numbers are all in MeV.

For $A = 8$, Amit and Katz do not include the (21) level at 16.62 MeV and the (11) level at 17.64 MeV excitation. Their parameters give both of these levels around 14.2 MeV above the ground state. In addition, they obtain 5 unobserved levels below the known second excited state of Be^8.

For $A = 10$ Amit and Katz omit the (40) level at 6.04 MeV above the ground state and their parameters would put it at 4.6 MeV. They do include a (01) level at 7.56 MeV and a (21) level at 8.9 MeV which the (8–16)2BME parameters would put at 12.0 MeV and 10.7 MeV, respectively. We omit the (01) level because it is likely [18]) to contain a large amount of (2s, 1d) admixture. We believe that inelastic electron scattering data indicate a (21) level near 7.5 MeV.

For $A = 11$ Amit and Katz omit the first excited state, the $(\frac{1}{2}\ \frac{1}{2})$ level at 2.14 MeV. They include the level at 6.81 MeV with a $\frac{3}{2}^-$ assignment, whereas experimental evidence indicates that it is a positive-parity state. Therefore we have not included it.

For $A = 12$ Amit and Katz do not include the first (20) level at 4.43 MeV excitation; their parameters place it at 5.8 MeV. They do include the (00) level at 7.65 MeV, which the parameters of the (8–16)2BME case place at 12.5 MeV. We have omitted this level because we believe it contains a large amount of (2s, 1d) admixture. This point is discussed in greater detail in the concluding section.

The (00) level of C^{12} and the (01) level discussed for B^{10} probably provide the main differences between the calculations. Since the experimental data are relatively sparse, a few levels can have a large influence on the result. It is just for this reason, that it is useful to have the added tests provided by the beta-decay and M1 data.

TABLE 7

Magnetic dipole moments (nuclear magnetons) calculated with the interaction of Amit and Katz

Nucleus	Magnetic dipole moments (n.m.)		
	Exp.	A.&K.	A.&K. (sign changed)
Li^8	+1.65	+0.52	−3.14
Be^9	−1.18	−0.92	−2.06
B^{10}	+1.80	+1.52	+2.27
B^{11}	+2.69	+2.42	+4.62
C^{13}	+0.70	+0.07	−1.33
N^{14}	+0.41	+0.36	+0.61

Column 3 results from the parameters of table 6; column 4 results from changing the signs of the matrix elements 6421 and 4210

An added benefit in considering the beta-decay and M1 data is that there is an ambiguity in the 2BME energy fits. Identical energy eigenvalues can be obtained by changing the signs † of the (64JT) and (42 JT) matrix elements of table 6. However, the resultant wave functions are much different, and one can choose between them by comparing calculated observables other than energy with experiment.

The M1 and beta-decay quantities have been calculated with the interaction of Amit and Katz. Large discrepancies between calculated values and experiment are found for either of sign for the (64JT) and (42JT) matrix elements. This is illustrated by the magnetic moments of the ground states (table 7). Our calculation gives a reasonably consistent picture for the prominent observed M1 and beta-decay quantities.

6. Resultant Two-Body Interactions

6.1. GENERAL FEATURES

The discussion of the two-body interaction is carried out most easily in the *LS* representation. Numerical values from the present calculation are given in table 8.

† This freedom is not present in the POT fits since the matrix elements are not independent.

In each column the diagonal matrix elements for a given (JT) differ by amounts which are large compared to the off-diagonal matrix elements. Also the even-state forces (even L, here) are strongly attractive whereas the odd-state forces are repulsive or weakly attractive. The important difference from the interaction of Amit and Katz [3]) is that these authors have a strongly attractive interaction for the odd-state $J = 0$, $T = 1$ integral; it is several times as great as their even-state interaction. This has a large effect on the wave functions of low-lying states and, together with the differences in the single-particle energies, accounts for the disagreements with the present calculation.

TABLE 8

Numerical values for $\langle LSJT|V|\overline{LS}JT\rangle$, the integrals of the two-body interaction in the LS representation

JT	LS	$\overline{LS}$	(8.16)POT	(8–16)2BME	(6–16)2BME
2 1	2 0	2 0	−2.38	−2.50	−3.06
	2 0	1 1	0	−0.27	−0.50
	1 1	1 1	+1.32	+1.38	+1.27
1 1	1 1	1 1	+0.73	+0.92	+0.86
0 1	0 0	0 0	−6.90	−6.80	−6.73
	0 0	1 1	0	−0.24	−0.33
	1 1	1 1	+3.82	+3.35	+4.33
3 0	2 1	2 1	−7.27	−7.23	−6.68
2 0	2 1	2 1	−4.06	−4.00	−4.23
1 0	2 1	2 1	−5.62	−5.64	−5.20
	2 1	0 1	−0.74	−1.05	−1.33
	2 1	1 0	0	−0.15	−0.73
	0 1	0 1	−8.38	−8.35	−8.81
	0 1	1 0	0	−0.56	−0.30
	1 0	1 0	−0.29	+0.05	+0.07

There are four non-diagonal matrix elements which vanish exactly in the POT case for reasons of spatial symmetry as discussed in sect. 2. For these integrals, the values extracted from the 2BME cases are rather small. The fact that they do not vanish in those cases may indicate that this extra freedom is being used to compensate for the restriction that no size variation of the nuclear wave functions is allowed in the fitting procedure. Some support for this view is found in the increased values of most of these integrals in going from the (8–16)2BME case to the (6–16)2BME case where the nuclear size variation is greater.

6.2. COMPONENTS OF THE POTENTIAL SOLUTION

The potential integrals can be analysed further in terms of the phenomenological potentials used to analyse nucleon-nucleon scattering. The form of the two-body potential is

$$V = V_{Cs}(\rho)P_s + V_{is}(\rho)(\boldsymbol{l}\cdot\boldsymbol{s}) + V_T(\rho)S_{12} + V_{Hs}(\rho)P_sH_{12}, \qquad (1)$$

where the V_i are functions of the separation $\rho = |r_1 - r_2|$. For $T = 1$ integrals, the V_i are the singlet-even and triplet-odd potentials, while for the $T = 0$ integrals the V_i are the singlet-odd and triplet-even potentials. The operators P_0 and P_1 are projection operators for the singlet and triplet spin states, respectively. The spin-orbit term couples the relative orbital angular momentum $\boldsymbol{l}$ to the total spin $\boldsymbol{s}$. The tensor operator S_{12} and the operator H_{12} are defined as

$$S_{12} = 3(\boldsymbol{\sigma}_1 \cdot \hat{\boldsymbol{\rho}})(\boldsymbol{\sigma}_2 \cdot \hat{\boldsymbol{\rho}}) - (\boldsymbol{\sigma}_1 \cdot \boldsymbol{\sigma}_2), \tag{2}$$
$$H_{12} = (a_0 - a_2)\{\tfrac{1}{3}(\boldsymbol{\sigma}_1 \cdot \boldsymbol{\sigma}_2)l^2\} + \tfrac{1}{2}a_2\{(\boldsymbol{\sigma}_1 \cdot \boldsymbol{l})(\boldsymbol{\sigma}_2 \cdot \boldsymbol{l}) + (\boldsymbol{\sigma}_2 \cdot \boldsymbol{l})(\boldsymbol{\sigma}_1 \cdot \boldsymbol{l})\}.$$

The term H_{12} was introduced by Hamada [19]) with $a_0 = 1 = a_2$ and later by Hamada and Johnson [20]) with the form $a_0 = +2$, $a_2 = -1$.

TABLE 9

Decomposition of the operators in eq. (1) into the form $\sum_m (-1)^m \mathscr{S}^{\mathscr{J}}_m(\boldsymbol{\sigma}_1, \boldsymbol{\sigma}_2)\mathscr{R}^{\mathscr{J}}_{-m}(\boldsymbol{\rho}, \boldsymbol{l})$

Operator	$\mathscr{J}$	$\mathscr{S}^{\mathscr{J}}_m$	$\mathscr{R}^{\mathscr{J}}_{-m}$
P_s	0	P_s	1
$l \cdot s$	1	s^1_m	l^1_{-m}
S_{12}	2	$[\boldsymbol{\sigma}_1, \boldsymbol{\sigma}_2]^2_m$	$3(\frac{8}{15}\pi)^{\frac{1}{2}} Y^2_{-m}(\Omega_\rho)$
H_{12}	0	$[\boldsymbol{\sigma}_1, \boldsymbol{\sigma}_2]^0_0$	$-a_0 l^2 (\frac{1}{3})^{\frac{1}{2}}$
	2	$[\boldsymbol{\sigma}_1, \boldsymbol{\sigma}_2]^2_m$	$a_2 l^2 (\frac{8}{15}\pi)^{\frac{1}{2}} Y^2_{-m}(\Omega_l)$

Here $[\boldsymbol{\sigma}_1, \boldsymbol{\sigma}_2]^{\mathscr{J}}_m$ represents vector coupling of $\boldsymbol{\sigma}_1$ and $\boldsymbol{\sigma}_2$ to a resultant $\mathscr{J}$.

Each of the operators which multiply the $V_i(\rho)$ can be written as a scalar constructed by coupling $\mathscr{S}^{\mathscr{J}}$ a tensor of rank $\mathscr{J}$ in the spin coordinates, to $\mathscr{R}^{\mathscr{J}}$, a tensor of rank $\mathscr{J}$ in the space coordinates; i.e., the scalar operator is $\sum_m (-1)^m \mathscr{S}^{\mathscr{J}}_m(\boldsymbol{\sigma}_1, \boldsymbol{\sigma}_2)$ $\mathscr{R}^{\mathscr{J}}_{-m}(\boldsymbol{\rho}, \boldsymbol{l})$. Explicit forms are given in table 9. The transformation properties of the tensors $\mathscr{S}^{\mathscr{J}}$ and $\mathscr{R}^{\mathscr{J}}$ then suffice to separate the contributions to the two-body integrals according to $\mathscr{J}$. In table 10 this has been done for the (8–16)POT case, and it is clear that the $\mathscr{J} = 0$ contributions are dominant. Only for the odd-state $T = 1$ integrals is there any competition from the $\mathscr{J} = 1$ and $\mathscr{J} = 2$ parts.

Finally, the spin-dependence can be evaluated numerically so that only the reduced matrix elements of the spatial coordinates are left. These matrix elements are collected in table 11 for the (8–16)POT case. This is the end product of the fit; any further interpretation requires assumptions about the $V_i(\rho)$.

Before we attempt interpretation, it is pertinent to ask how well the numerical values of table 11 are determined by the energy fit. The minimum in χ^2 is not sharp and it would be misleading merely to quote how much χ^2 changes as a given parameter is changed. This is because there are correlations in the sense that appreciable

TABLE 10

Contributions to the integrals $\langle LSJT|V_{\mathscr{J}}|\bar{L}\bar{S}JT\rangle$, separated according to $\mathscr{J}$ for the (8–16)POT case

JT	LS	$\bar{L}\bar{S}$	$\mathscr{J}=0$ (central and a_0 part of V_H)	$\mathscr{J}=1$ (spin-orbit)	$\mathscr{J}=2$ (tensor and a_2 part of V_H)
2 1	2 0	2 0	−2.38	0	0
	1 1	1 1	−1.40	−0.27	−0.19
1 1	1 1	1 1	−1.40	−0.27	−0.94
0 1	0 0	0 0	−6.90	0	0
	1 1	1 1	−1.40	−0.54	−1.88
3 0	2 1	2 1	5.87	−1.03	−0.37
2 0	2 1	2 1	−5.87	+0.51	−1.30
1 0	2 1	2 1	−5.87	−1.54	−1.30
	2 1	0 1	0	0	−0.74
	0 1	0 1	−8.38	0	0
	1 0	1 0	−0.29	0	0

TABLE 11

Numerical values (in MeV) of the spatial reduced matrix elements of the potential in eq. (1)

$T=1$ (singlet-even, triplet-odd)

$$\langle \mathrm{S}\|V_{\mathrm{C0}}^{+}(\rho)+\sqrt{3}V_{\mathrm{H0}}^{+}(\rho)R^{0}(l)\|\mathrm{S}\rangle = -6.90$$
$$\langle \mathrm{D}\|V_{\mathrm{C0}}^{+}(\rho)+\sqrt{3}V_{\mathrm{H0}}^{+}(\rho)R^{0}(l)\|\mathrm{D}\rangle = -2.38$$
$$\langle \mathrm{P}\|V_{\mathrm{C1}}^{-}(\rho)-\tfrac{1}{3}\sqrt{3}V_{\mathrm{H1}}^{-}(\rho)R^{0}(l)\|\mathrm{P}\rangle = +1.40$$
$$\langle \mathrm{P}\|V_{ls}^{-}(\rho)l^{1}\|\mathrm{P}\rangle = -0.38$$
$$\langle \mathrm{P}\|V_{\mathrm{T}}^{-}(\rho)R^{2}(\rho)+V_{\mathrm{H1}}^{-}(\rho)R^{2}(l)\|\mathrm{P}\rangle = +0.73$$

$T=0$ (singlet-odd, triplet-even)

$$\langle \mathrm{S}\|V_{\mathrm{C1}}^{+}(\rho)-\tfrac{1}{3}\sqrt{3}V_{\mathrm{H1}}^{+}(\rho)R^{0}(l)\|\mathrm{S}\rangle = -8.38$$
$$\langle \mathrm{D}\|V_{\mathrm{C1}}^{+}(\rho)-\tfrac{1}{3}\sqrt{3}V_{\mathrm{H1}}^{+}(\rho)R^{0}(l)\|\mathrm{D}\rangle = -5.87$$
$$\langle \mathrm{P}\|V_{\mathrm{C0}}^{-}(\rho)+\sqrt{3}V_{\mathrm{H0}}^{-}(\rho)R^{0}(l)\|\mathrm{P}\rangle = -0.29$$
$$\langle \mathrm{D}\|V_{ls}^{+}(\rho)l^{1}\|\mathrm{D}\rangle = -1.26$$
$$\langle \mathrm{D}\|V_{\mathrm{T}}^{+}(\rho)R^{2}(\rho)+V_{\mathrm{H1}}^{+}(\rho)R^{2}(l)\|\mathrm{D}\rangle = -0.85$$
$$\langle \mathrm{D}\|V_{\mathrm{T}}^{+}(\rho)R^{2}(\rho)+V_{\mathrm{H1}}^{+}(\rho)R^{2}(l)\|\mathrm{S}\rangle = -0.29$$

The form is $\langle L\|V(P)\mathscr{R}^{\mathscr{J}}\|\bar{L}\rangle$, where L is the orbital wave function of two 1p nucleons and $\mathscr{R}^{\mathscr{J}}$ is an operator from table 9. $\langle LM|V(P)\mathscr{R}^{\mathscr{J}}_{\mathscr{J}_z}|\bar{L}\bar{M}\rangle = (L\,\mathscr{J}\,\bar{M}\,\mathscr{J}_z|LM)\langle L\|V(P)\mathscr{R}^{\mathscr{J}}\|\bar{L}\rangle$.

simultaneous changes in several parameters may give only a slight change in χ^2. The best we can do is to study the way the minimum is approached in calculations starting from several different sets of input parameters and to give a qualitative idea of how well the final values of the parameters are determined.

The best-determined integrals are those involving the even-state central forces. This is not surprising since these make the major contributions to the two-body integrals of table 10. The values of these four integrals are determined to about 10 %. At the other extreme are the integrals involving the tensor force and the singlet-odd central force. The signs and magnitudes appear to be determined for the integrals with the tensor force, but some particular changes by as much as 50 % still leave reasonable fits. The singlet-odd integral is the least important parameter since it varies between +0.5 and −3.5 and is for practical purposes undetermined.

This leaves the triplet-odd central integral and the integrals of the spin-orbit force which lie between these extremes. Although the spin-orbit integrals seem fairly well determined, they have effects similar to those of the separation of the $1p_{\frac{1}{2}}$ and $1p_{\frac{3}{2}}$ single-particle levels. While the $1p_{\frac{3}{2}}$ energy is well determined, the $1p_{\frac{1}{2}}$ energy is an insensitive parameter, and its position affects the values of the spin-orbit integrals.

Thus the interaction of table 11 contains the important features of the effective interaction in the 1p shell, but certain features indicated above are quite pooly determined.

6.3. INTERPRETATION OF THE POTENTIAL SOLUTION

Although there is no compelling reason for believing that the effective interaction of the 1p nucleons should resemble the interaction derived from scattering experiments, it is interesting to make a comparison. This requires a form for the radial 1p functions. The ones chosen were the harmonic-oscillator functions since these facilitate the extraction of the dependence on the relative coordinates of the two nucleons. This suffices for a qualitative picture, which is all that is appropriate in view of the uncertainty of the numerical values in table 11.

The use of the harmonic-oscillator functions makes it easy to evaluate the effects of the operators $\mathscr{R}^J(\rho, l)$ for the integrals of table 11. What remains is a set of radial integrals in the relative coordinate ρ, involving only the dependence on the various $V_i(\rho)$ appearing in the potential of eq. (1). These integrals are the Talmi integrals [21]) or linear combinations thereof. The expressions together with numerical values from the (8–16)POT case are listed in table 12, where they are grouped according to spin and parity. Within each group they are ordered according to which of the $V_i(\rho)$ are most important in the phenomenological nucleon-nucleon interaction. For those $V_i(\rho)$ that occur in only one integral, one can only compare the sign and rough magnitude with what is found in the analysis of scattering. In the singlet-even and triplet-even case, one can in addition say something about the range.

In the following paragraphs, each group will be compared with the general features of the potential constructed by Hamada and Johnston [20]) to fit nucleon-nucleon

scattering below 300 MeV. In this potential, the constants in H_{12} of eq. (2) are $a_0 = +2$, $a_2 = -1$; this is the major difference from the earlier potential used by Brueckner, Gammel and Thaler [22]) which had $a_0 = 0 = a_2$. The important differences between the HJ and BGT potentials occur in the triplet states and will be noted in the following comparison.

TABLE 12

Numerical values of the radial integrals from the (8–16)POT case in relative coordinates

Singlet-even	
$\langle 1s\|V_{C0}^{+}\|1s\rangle + \langle 2s\|V_{C0}^{+}\|2s\rangle$	$= -13.80$
$\langle 1s\|V_{C0}^{+}\|1s\rangle + \langle 1d\|V_{C0}^{+} - 6a_0 V_{H0}^{+}\|1d\rangle$	$= -4.76$
Triplet-odd	
$\langle 1p\|V_{T}^{-} - \frac{5}{6}a_2 V_{H1}^{-}\|1p\rangle$	$= +0.94$
$\langle 1p\|V_{ls}^{-}\|1p\rangle$	$= -0.54$
$\langle 1p\|V_{C1}^{-} + \frac{2}{3}a_0 V_{H1}^{-}\|1p\rangle$	$= +1.40$
Triplet-even	
$\langle 1s\|V_{C1}^{+}\|1s\rangle + \langle 2s\|V_{C1}^{+}\|2s\rangle$	$= -16.76$
$\langle 1s\|V_{C1}^{+}\|1s\rangle + \langle 1d\|V_{C1}^{+} + 2a_0 V_{H1}^{+}\|1d\rangle$	$= -11.74$
$\langle 1d\|V_{T}^{+} - \frac{7}{2}a_2 V_{H1}^{+}\|1d\rangle$	$= +1.30$
$\langle 1d\|V_{Ten}^{+}\|2s\rangle$	$= -0.52$
$\langle 1d\|V_{ls}^{+}\|1d\rangle$	$= -1.03$
Singlet-odd	
$\langle 1p\|V_{C0}^{-} - 2a_0 V_{H0}^{-}\|1p\rangle$	$= -0.29$

Harmonic-oscillator functions are assumed for the 1p nucleons. The form is $\langle nl|V_i(\rho)|\bar{n}\bar{l}\rangle$, where $|nl\rangle$ denotes the radial oscillator function $R_{nl}(m\omega\rho^2/2\hbar)$. For $n = \bar{n}$ and $l = \bar{l}$, these are the Talmi integrals.

The singlet-even part of the HJ potential is dominated by an attractive central potential V_{C0}^{+} of fairly long range and gives V_{H0}^{+} as weak and attractive with very short range. The integrals of table 12 also indicate a strong attractive V_{C0}^{+}. However if V_{H0}^{+} is weak, the numerical values of the V_{C0}^{+} integrals indicate a very short range dependence. This effective interactions appears to be very much like a pairing interaction.

The triplet-odd part of the HJ potential consists chiefly of a repulsive tensor potential V_{TEN}^{-} of fairly long range and an attractive spin-orbit potential V_{ls}^{-} of shorter range. The central potential V_{C1}^{-} is very weak and attractive while V_{H1}^{-} is attractive and of very short range. The BGT potential does not contain V_{ls}^{-} or V_{H1}^{-}, but the

remaining features are like those of the HJ potential. The integrals of table 12 also indicate a repulsive V_T^- and an attractive V_{ls}^-, in agreement with the major part of the triplet-even component of the HJ potential. However, the integrals indicate that $(V_{C1}^- + \frac{2}{3}a_0 V_{H1}^-)$ is repulsive – in disagreement with that feature for both the HJ and BGT potentials. While the magnitude of the integral that shows a repulsive contribution is less definite, the sign appears to be the same in all the fits.

The triplet-even part of the HJ potential is dominated by a long-range attractive tensor part V_T^+ and an attractive fairly long-range central V_{C1}^+. In addition, there is a shorter range repulsive V_{H1}^+ and a weak repulsive V_{ls}^+. The BGT potential has the same sort of V_T^+ and V_{C1}^+, but no V_{H1}^+ and a very short-range attractive V_{ls}^+. The integrals of table 12 suggest a strong attractive V_{C1}^+. If one were to assume $a_2 V_{H1}^+ = 0$, the tensor integrals would lead to a very long-range repulsive V_T^+ in contradiction to the prominent attractive nature of V_T^+ in the scattering potentials. However, since the 1d integral contains the combination $(V_T^+ + \frac{7}{2}V_{H1}^+)$ for the HJ potential, the contribution from the repulsive V_{H1}^+ can outweigh the contribution from an attractive V_T^+. With the sort of relative magnitudes of V_{H1}^+ and V_T^+ given by the HJ potential, one can satisfy the requirements of the integrals in table 12 with a moderately long-range attractive V_T^+. Therefore these integrals are consistent with the strong features of the HJ potential but not the BGT potential. The spin-orbit integral indicates an attractive V_{ls}^+, in contradiction to the weak repulsive V_{ls}^+ of the HJ potential.

The singlet-odd integral will not be discussed since it is so poorly determined that the sign is uncertain. It is a weak part of the scattering potentials.

From the comparison one sees that the integrals of table 12 are consistent with the main features of the HJ potential as far as signs and magnitudes are concerned. There are disagreements with the range of V_{C0}^+, the sign of the contribution $(V_{C1}^+ + \frac{2}{3}a_0 V_{H1}^-)$, and the sign of V_{ls}^+. However, an over-all similarity between the effective interaction and the HJ potential is evident.

7. Summary and Conclusions

We have attempted to derive single-particle energies and an effective interaction for the 1p shell by fitting observed energy levels. The parameters were assumed to be constant over the range of nuclei under consideration. This is a severe restriction, particularly if we include the lower end of the shell where both the size of the 1p orbitals and the effective interaction with the $(1s)^4$ core probably change appreciably with the number of 1p nucleons. Such changes would affect the integrals of the effective interaction and the single-particle energies which contain the effective interaction with the $(1s)^4$ core. This is the probable explanation of the markedly poorer over-all fit obtained when the lower end of the shell is included.

If one somewhat arbitrarily omits the data for $A = 6$ and 7, a fit with a general potential form is nearly as good as if one allows completely free integrals of the two-body interaction. Furthermore the resultant spectra for $A = 6$ and 7 are still roughly

similar to observation. The general features of the resultant potential are consistent in signs and magnitudes with the dominant features of the potential constructed by Hamada and Johnston from nucleon-nucleon scattering data below 300 MeV. In particular, the 1p potential indicates the need for the term H_{12} of eq. (2) in the triplet-even interaction. Nevertheless, there are points of disagreement in the comparison with the Hamada-Johnston potential.

The end result of the energy fit is the set of radial reduced matrix elements of table 11. If one assumes a harmonic-oscillator form for the radial 1p function, the integrals can be transformed to the Talmi integrals of table 12. There have been interesting studies [23, 24]) wherein the Talmi integrals for the 1p shell were approximated in calculations starting with potentials from nucleon-nucleon scattering. It should prove mutually beneficial to compare those values with results of calculations, such as the present one, in which one finds numerical values of the integrals by comparison with the energy-level data.

Since the number of pieces of information on energy levels is not very large compared with the number of parameters, the results can depend markedly on which levels are included as arising mainly from 1p configurations. The comparison of our results with those obtained by Amit and Katz demonstartes this point. The prominent level we have omitted is the $(0^+, T = 0)$ level seen at 7.65 MeV in C^{12}. Our calculations give a (0 0) excited state about 5-6 MeV higher.

The picture we suggest for the observed state is that it consists partly of the calculated excited (0 0) from the 1p configuration together with a large part coming from exciting two nucleons to the (2s 1d) shell. This interpretation gains its plausibility from the Nilsson picture for levels in a deformed potential. For oblate deformation in this mass region, two close low-lying 1p levels are filled to give the ground-state band [25]) of C^{12}. Then for large deformation there is an appreciable gap followed by four Nilsson levels: one from the 1p shell and three from the (2s 1d) shell. The excited (0 0) level given by the fit can be represented by raising one or more nucleons from the low-lying 1p levels to the upper 1p level. However it may be just as advantageous to raise pairs of nucleons to any one of the upper group of four levels and then include a coherent interaction (such as the pairing interaction) to produce a lowered (0 0) state. This coherent state, which would contain mostly $(2s\ 1d)^2$, can then mix with the state produced by exciting a single 1p nucleon from the lower levels to give the observed 7.65 MeV state. Such a picture can account for the observed beta decay of B^{12} which gives [6]) $\log ft = 4.2 \pm 0.3$ for decay to the 7.65 MeV state. In table 4 one finds that $\log ft \approx 3.5$ for decay to the calculated excited (0 0) state. Therefore inclusion of even a minor amount of this state will give the allowed beta decay.

The evidence on magnetic moments, M1 transitions and Gamow-Teller beta decays has been shown to be an important test of the nature of the 1p wave functions resulting from the energy fits. Tables 3–5 show that the wave functions usually are not too different from those obtained in earlier intermediate-coupling calculations with a much different interaction. The changes that do occur indicate that the present inter-

action gives better agreement with experiment. A few points of particular experimental interest, such as the encouraging result for the beta decay of C^{14}, were pointed out in sect. 4. Some features appear to be very sensitive to the wave functions. Is it clear that inclusion of the well-determined information about these other observables together with energy data would be desirable in trying to determine an effective 1p-shell interaction more definitely.

However, there is clearly a limit as to how far one can push this procedure. The data are quite insensitive to certain features of the interaction; changing such parameters by large amounts to obtain a slightly better over-all fit to experiment can hardly be physically meaningful. The assumption of pure 1p configurations is clearly less valid near the upper end of the shell, and the effect of (2s 1d) admixture will have to be included. It is perhaps surprising that the pure 1p picture works as well as it does.

The authors would like to point out that this study would not have been possible without the extensive shell-model codes. These programs were developed in conjunction with R. D. Lawson, M. H. Macfarlane and M. Soga, whom we would also like to thank for general consultation.

References

1) J. P. Elliott and A. M. Lane, Handbuch der Physik, Vol. 39 (Springer-Verlag, Berlin, 1957) p. 336
2) S. Meshkov and C. W. Ufford, Phys. Rev. **101** (1956) 734;
S. Goldstein and I. Talmi, Phys. Rev. **102** (1956) 589;
S. P. Pandya, Phys. Rev. **103** (1956) 956
3) D. Amit and A. Katz, Nuclear Physics **58** (1964) 388
4) S. Cohen, R. D. Lawson, M. H. Macfarlane and M. Soga, Phys. Lett. **9** (1964) 180
5) W. C. Davidon, Argonne National Laboratory Report ANL-5990 Rev. (1959) unpublished
6) F. Ajzenberg-Selove and T. Lauritsen, Nuclear Physics **11** (1959) 1;
Energy levels of light nuclei National Academy of Sciences–National Research Council (May, 1962)
7) D. E. Alburger, Phys. Rev. **132** (1963) 328
8) A. Marques, A. J. P. L. Policarpo and W. R. Philips, Nuclear Physics **36** (1962) 45
9) D. Kurath, Phys. Rev. **101** (1956) 216; **106** (1957) 975
10) D. R. Inglis, Revs. Mod. Phys. **25** (1953) 390
11) V. Meyer, H. Müller, H. H. Staub and R. Zurmühle, Nuclear Physics **27** (1961) 284
12) R. D. Edge and G. A. Peterson, Phys. Rev. **128** (1932) 2750
13) D. H. Wilkinson, private communication
14) D. H. Wilkinson and D. E. Alburger, Phys. Rev. **113** (1959) 563
15) I. Talmi and I. Unna, Phys. Rev. Lett. **4** (1960) 469
16) H. Schmid and W. Scholz, Z. Phys. **175** (1963) 430; F. Gudden, Phys. Lett. **10** (1964) 313
17) F. C. Barker, G. D. Symons, N. W. Tanner and P. B. Treacy, Nuclear Physics **45** (1963) 449; F. C. Barker, Nuclear Physics **45** (1963) 467
18) W. W. True and E. K. Warburton, Nuclear Physics **22** (1961) 426
19) T. Hamada, Prog. Theor. Phys. **24** (1960) 1033, **25** (1961) 247
20) T. Hamada and I. D. Johnston, Nuclear Physics **34** (1962) 382
21) I. Talmi, Helv. Phys. Acta **25** (1952) 185
22) K. A. Brueckner and J. L. Gammel, Phys. Rev. **109** (1958) 1023
23) N. Meshkov, Nuclear Physics **35** (1962) 485
24) J. F. Dawson and J. D. Walecka, Ann. of Phys. **22** (1963) 133
25) D. Kurath and L. Picman, Nuclear Physics **10** (1959) 313